JCTC Journal of Chemical Theory and Computation

Quantum Chemical Modeling of the Dehalogenation Reaction of Haloalcohol Dehalogenase

Kathrin H. Hopmann and Fahmi Himo*

Department of Theoretical Chemistry, School of Biotechnology, Royal Institute of Technology, AlbaNova University Center, SE-106 91 Stockholm, Sweden

Received February 12, 2008

Abstract: The dehalogenation reaction of haloalcohol dehalogenase HheC from *Agrobacterium radiobacter* AD1 was investigated theoretically using hybrid density functional theory methods. HheC catalyzes the enantioselective conversion of halohydrins into their corresponding epoxides. The reaction is proposed to be mediated by a catalytic Ser132−Tyr145−Arg149 triad, and a distinct halide binding site is suggested to facilitate halide displacement by stabilizing the free ion. We investigated the HheC-mediated dehalogenation of (*R*)-2-chloro-1-phenylethanol using three quantum chemical models of various sizes. The calculated barriers and reaction energies give support to the suggested reaction mechanism. The dehalogenation occurs in a single concerted step, in which Tyr145 abstracts a proton from the halohydrin substrate and the substrate oxyanion displaces the chloride ion, forming the epoxide. Characterization of the involved stationary points is provided. Furthermore, by using three different models of the halide binding site, we are able to assess the adopted modeling methodology.

I. Introduction

Haloalcohol dehalogenases (also known as halohydrin dehalogenases, halohydrin epoxidases, or hydrogen-halide lyases) are microbial enzymes that catalyze the reversible dehalogenation of vicinal haloalcohols, thereby forming the corresponding epoxides (Scheme 1). Haloalcohol dehalogenase activity has been identified in multiple microbial sources, including *Corynebacterium* sp.,[1] *Arthrobacter* sp.,[2,3] *Agrobacterium* radiobacter,[3] and *Mycobacterium* sp.[3] During recent years, haloalcohol dehalogenases have acquired increasing interest. It has been realized that they are of importance for the degradation of various halogenated environmental pollutants.[4] In addition, they have received recognition as promising biocatalysts that can be used for the kinetic resolution of epoxides and halohydrins, and for the preparation of various substituted alcohols.[5] Haloalcohol dehalogenases have broad substrate specificities, and in addition to the dehalogenation reaction, they are also able to catalyze the irreversible ring-opening of epoxides with the nonhalide nucleophiles NO_2^-, CN^-, and N_3^-.[5–11]

Sequence alignments suggested that the haloalcohol dehalogenases are structurally and mechanistically similar to the family of short-chain dehydrogenases/reductases (SDRs).[3] SDRs exhibit a conserved catalytic Ser−Tyr−Lys/(Arg) triad that also can be identified in haloalcohol dehalogenases.[3] However, the reactions catalyzed by the two families are very different. SDRs catalyze NAD(P)H-dependent oxidation and reduction reactions, while the haloalcohol dehalogenases catalyze a cofactor-independent dehalogenation reaction.

Scheme 1. Haloalcohol Dehalogenase Reaction

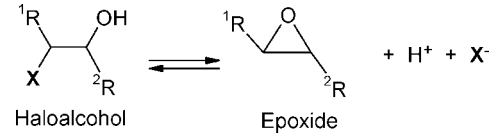

Determination of the crystal structure of the haloalcohol dehalogenase HheC from *Agrobacterium radiobacter* AD1 confirmed structural similarities to the SDRs.[12] However, instead of the NAD(P)H binding site found in SDRs, the structure of HheC revealed a distinct halide binding site.[12] The putative catalytic triad, Ser132−Ty145−Arg149, is positioned above the halide binding site (Figure 1). This supports the proposed mechanism shown in Scheme 2.[3,12] Tyr145 is proposed to be the catalytic base that abstracts a proton from the halohydrin substrate. The substrate oxyanion

* Corresponding author e-mail: himo@theochem.kth.se.

10.1021/ct8000443 CCC: $40.75
Published on Web 06/13/2008

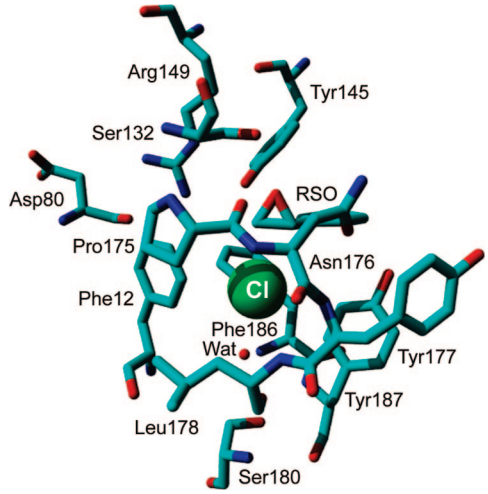

Figure 1. Active site of HheC (from the X-ray crystal structure of HheC in complex with (*R*)-styrene oxide and chloride, PDB: 1PWZ).[12] The chloride ion is shown in ball representation.

then displaces the chloride ion through an intramolecular S_N2 reaction. Arg149 is suggested to activate Tyr145 by abstracting a proton. Ser132 seems to be of importance for binding of the substrate as well as for stabilization of the emerging oxyanion.[3,12] Also, the conserved residue Asp80 has been shown to be of importance for the activity of HheC,[12] as its backbone carbonyl interacts with Arg149 and might be important for its positioning. Additionally, the Asp80 carboxyl side chain is proposed to be involved in a proton transfer pathway, which removes excess protons from the active site.[12] The displaced chloride ion is stabilized through interactions in the halide binding site. The crystal structures of HheC in complex with either bromide or chloride reveal several distinct interactions that seem to stabilize the free halide.[12] These include hydrogen-bonding interactions with the backbone amides of Tyr177 and Leu178, as well as with an ordered water molecule. Other residues suggested to be important for the formation of the halide binding site are Phe12, Pro175, Asn176, Phe186, and Tyr187 (Figure 1).[12]

It is today a quite common procedure to use relatively small models of enzyme active sites and apply quantum chemical methods to study their reaction mechanisms.[13] In this approach, the rest of the enzyme is usually treated using a homogeneous polarizable medium with some assumed dielectric constant. Density functional theory (DFT), and in particular the B3LYP functional,[14] has become the method of choice in this kind of study. It has been shown in many examples that the calculated energies often are sufficient to verify or rule out a suggested reaction mechanism, and in general, the experience has been that a well-chosen quantum model is able reproduce the chemistry taking place at an enzyme active site to such a high degree that it can provide detailed insight into mechanisms and selectivities.[15]

In the present study, we use this approach to examine the reversible dehalogenation reaction of the haloalcohol dehalogenase HheC. The transformation of (*R*)-2-chloro-1-phenylethanol to yield the epoxide (*R*)-styrene oxide (RSO) is studied with HheC active site models of different sizes. In similar studies, we have previously investigated the reaction mechanisms of two epoxide-hydrolyzing enzymes, namely, limonene epoxide hydrolase[16] and soluble epoxide hydrolase.[17] These investigations have established the adequacy of this approach to study mechanisms of this kind. However, the current HheC case presents an additional challenge in that a free halide ion is released at the active site. It is not *a priori* evident that a relatively small quantum chemical active site model, in conjunction with implicit solvation models, will be sufficient to describe the energetics of this system correctly. Previous calculations on other enzymatic dehalogenation reactions have generally employed molecular dynamics, quantum mechanics/molecular mechanics (QM/MM), or semiempirical methods.[18] We chose instead to study the reaction of HheC with the more accurate B3LYP method. This, however, puts some limitations on the size of the models that can be employed. Here, we have constructed and compared three different models of the HheC active site. The aim of the study is to shed more light on the dehalogenation reaction mechanism of HheC and also to assess the applicability of the adopted methodology.

II. Computational Details

All calculations were performed using the hybrid density functional theory method B3LYP,[14] as implemented in Gaussian 03.[19] Geometries were optimized with the 6-31G(d,p) basis set. On the basis of these geometries, more accurate energies were calculated by performing single-point calculations using the 6-311+G(2d,2p) basis set. Basis set superposition errors were not explicitly considered in this study.

For Model A (see below), zero-point vibrational (ZPV) energies were calculated by performing frequency calculations on the optimized structures at the same level as optimizations. The size of Models B and C (see below) did not permit the calculation of frequencies. Instead, the ZPV effects were transferred from Model A. The solvation corrections were calculated at the same level of theory as optimizations by performing single-point calculations using the conductor-like polarizable continuum model (CPCM).[20] The energies presented here are the large basis set energies corrected for ZPV effects.

To preserve the overall spatial conformation of the models, the truncation points of residues included in the active site models were kept fixed to their X-ray positions during the geometry optimizations. This procedure gives rise to a number of small imaginary frequencies, typically around eight of them, all below $70i$ cm^{-1}. These frequencies do not contribute significantly to the zero-point energies and can thus be tolerated. However, they render the calculated harmonic entropy contributions unreliable. Thus, the reported energies here correspond to the enthalpies only.

III. Results and Discussion

III.a. Model A. We first devised a model of the HheC active site consisting of 83 atoms (called Model A). It was built on the basis of the crystal structure of HheC in complex with (*R*)-styrene oxide and chloride (PDB: 1PWZ; 2.50Å resolution).[12] The model contains parts of the side chains of the suggested Arg149−Tyr145−Ser132 catalytic triad and the backbone carbonyl of Asp80, which interacts with

Scheme 2. Proposed Dehalogenation Mechanism of HheC[3,12]

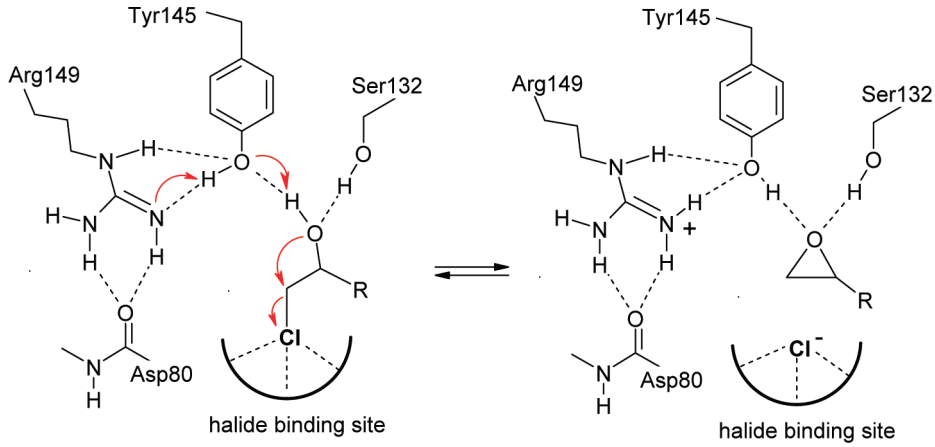

Arg149. A very small model of the halide binding site was used, consisting of the backbone of Leu178, parts of Phe186, and the crystallographically observed water molecule (Figure 2). As a substrate, we used (*R*)-2-chloro-1-phenyl-ethanol (RCPE). The dehalogenation of RCPE results in the formation of RSO and free chloride, corresponding to the complex observed in the 1PWZ X-ray crystal structure of HheC.[12]

As suggested from the proposed mechanism (Scheme 2), Arg149 and Tyr145 were modeled in their neutral forms. However, calculations showed that a more stable structure would be obtained if the two residues instead were modeled as protonated Arg149 and deprotonated Tyr145 ($Arg^{+}-Tyr^{-}$). For Model A, the charge-separated reactant was calculated to be 3.0 kcal/mol (using $\epsilon = 4$) lower in energy than the reactant with a neutral Arg−Tyr pair and was thus taken as the starting point for our investigation of the dehalogenation reaction. It can be noted in this context that the optimum pH of HheC for the dehalogenation reaction is between pH 8 and 9.[12] This is in line with a scenario in which a protonated Arg149 residue stabilizes an anionic Tyr145. In contrast, the reverse epoxide-opening reaction of HheC has a pH optimum of around 4−5,[12] indicating that both residues would be protonated in this case, allowing Tyr145 to function as a catalytic acid instead.

In the optimized reactant structure of Model A with RCPE (Figure 2B), the hydroxyl group of the substrate interacts with Tyr145 and Ser132. The chloro substituent is hydrogen-bonded to the amide backbone of Leu178 and to the water molecule.

Starting from this structure, we have located the transition state for the dechlorination reaction (shown in Figure 2C). The reaction turns out to occur in one single concerted step in which the alcohol proton is transferred to the phenolate of Tyr145, the alcohol oxygen performs a nucleophilic attack at the vicinal carbon, and the chlorine is displaced. Important optimized bond distances are displayed in Figure 2C. The O−C distance is 1.80 Å, and the C−Cl distance is 2.51Å. The alcohol proton is 1.04 Å from Tyr145 and 1.42 Å from the substrate oxygen. The hydrogen bond between Ser132 and the substrate oxygen is only slightly shorter than in the reactant structure. The hydrogen bonds from water and the Leu178 amide to the chloride are shortened significantly, from 3.44 and 4.25 Å, respectively, in the reactant to 3.20 and 3.63 Å at the transition state (hydrogen-bond length refers here to the distance from donor to acceptor atom).

In the product state with (*R*)-styrene oxide, the proton from the substrate has been fully transferred to Tyr145 (Figure 2D). The chloride ion remains hydrogen-bonded to water and the amide nitrogen. The lengths of the two hydrogen bonds have shortened further to 3.13 and 3.25 Å, respectively.

Without the inclusion of solvation effects, the calculated barrier for this reaction is 23.0 kcal/mol and the reaction energy is +17.5 kcal/mol (Table 1). From Figure 2C and D, it is seen that, despite the two hydrogen bonds, the chlorine ion appears quite exposed in the transition state and product structure of Model A. This suggests that the inclusion of solvation will have pronounced effects on the calculated energetics.

To account for the parts that are not explicitly included in the model, we have, as a first approximation, assumed that the surrounding is a homogeneous polarizable medium. This approximation has been used frequently in combination with quantum chemical active site models.[13,15] The solvation energies were computed using the CPCM method[20] on the optimized geometries. The choice of the dielectric constant is somewhat arbitrary, but the value $\epsilon = 4$ is frequently used in similar studies. In the present study, we chose to compare five different dielectric constants ($\epsilon = 2$, 4, 8, 16, and 80) to investigate the influence of the choice on the energetics. The calculated energies are presented in Table 1. As expected, solvation effects lower the energies of both the transition state and the product structures compared to the reactant. The barrier decreases from 23.0 kcal/mol without solvation to 15.0 and 12.2 kcal/mol using $\epsilon = 4$ and $\epsilon = 80$, respectively. The effect on the reaction energy is even more pronounced, resulting in a decrease from +17.5 kcal/mol without solvation to +3.4 and −1.2 kcal/mol using $\epsilon = 4$ and $\epsilon = 80$, respectively.

The experimentally determined rate constant for the HheC-catalyzed dehalogenation of RCPE is 48.5 s^{-1}.[3] Using classical transition state theory, this rate can be converted to a barrier of ca. 15 kcal/mol. It has been shown that halide release is rate-limiting in HheC.[21] It can thus be concluded that the barrier for the chemical step should be equal to or less than 15 kcal/mol. In addition, it has been shown experimentally that the equilibrium of HheC

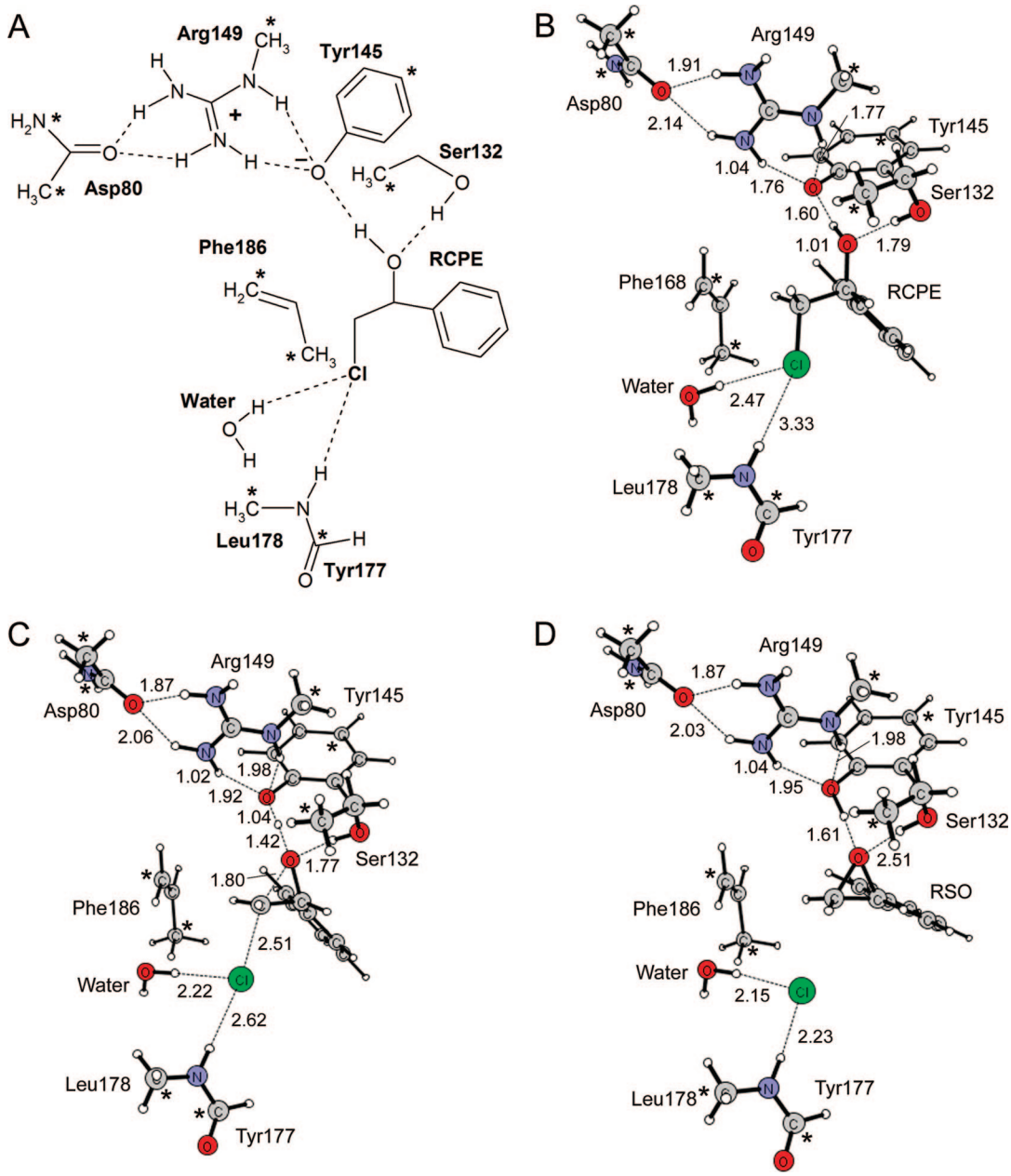

Figure 2. Optimized geometries for the formation of (*R*)-styrene oxide (RSO) from (*R*)-2-chloro-1-phenyl-ethanol (RCPE) in HheC active site Model A. (A) Schematic representation of the model. (B) Reactant geometry. (C) Transition state. (D) Product geometry. Distances are in ångstroms. Asterisks indicate atoms that are kept fixed to their crystallographically observed positions in calculations.

Table 1. Summary of the Calculated Energetics (kcal/mol) for the HheC-Catalyzed Transformation of RCPE to RSO

	Model A (83 atoms)		Model B (112 atoms)		Model C (161 atoms)	
	barrier	reaction energy	barrier	reaction energy	barrier	reaction energy
no solvation	23.0	+17.5	17.9	+14.1	18.2	+5.5
$\epsilon = 2$	17.8	+8.2	15.8	+8.3	17.7	+4.9
$\epsilon = 4$	15.0	+3.4	14.6	+5.2	17.4	+4.5
$\epsilon = 8$	13.5	+1.0	14.0	+3.6	17.1	+4.3
$\epsilon = 16$	12.8	−0.3	13.7	+2.8	17.0	+4.2
$\epsilon = 80$	12.2	−1.2	13.5	+2.2	17.0	+4.2

with styrene oxides and chloride is toward epoxide formation.[7] When (*R*)-*p*-nitrostyrene oxide and NaCl were used, the equilibrium constant K_{eq} = [NaCl] × [epoxide]/[chloroalcohol] was measured to be 40 mM.[7] From this, it can be concluded that the reaction should be exothermic. A similar conclusion can be reached considering the fact that HheC was successfully cocrystallized with RSO and chloride,[12] indicating that the enzyme-bound product state is energetically more favorable than the reactant state with the haloalcohol bound.

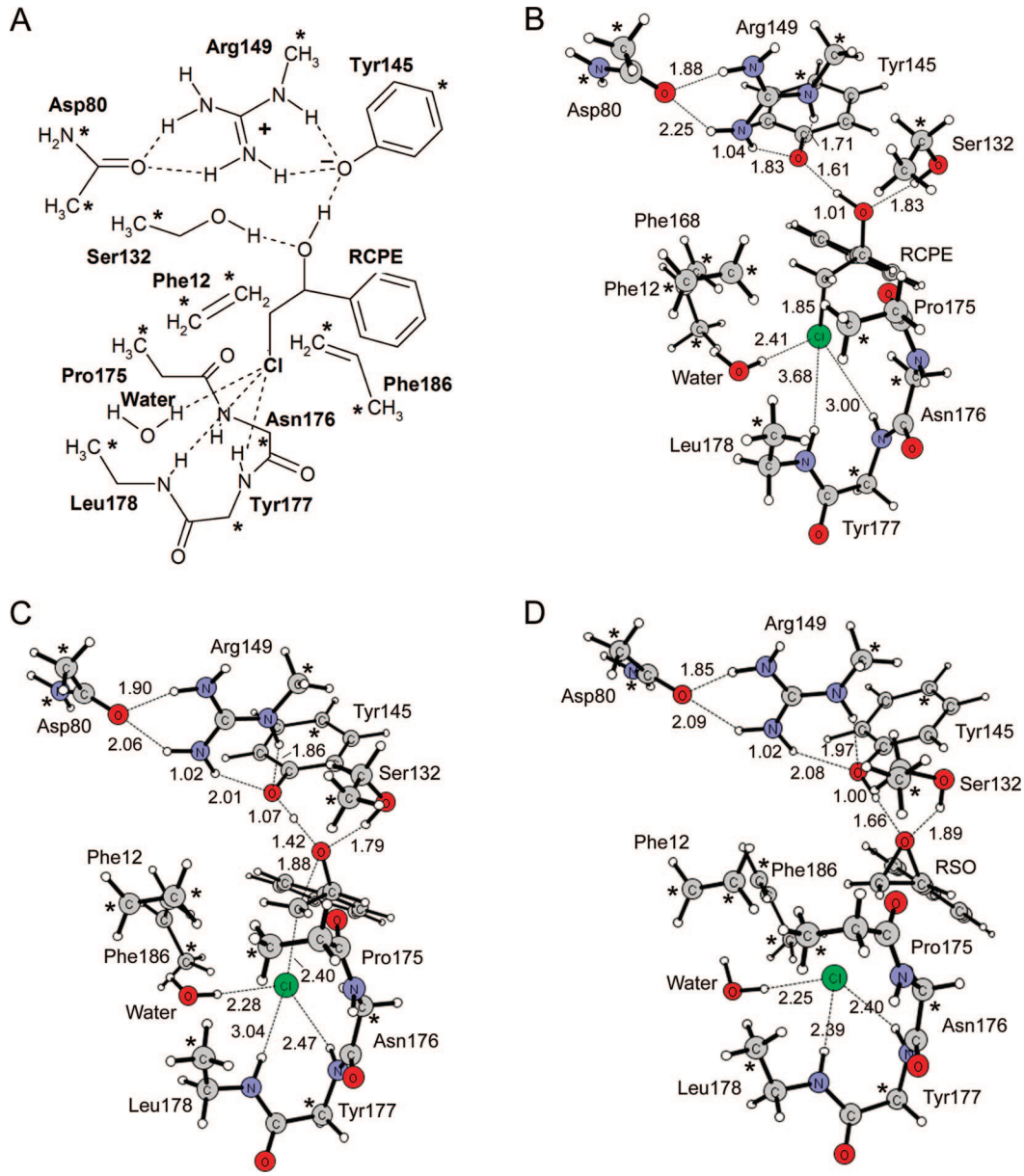

Figure 3. Optimized geometries for Model B. (A) Schematic representation of the model. (B) Reactant geometry. (C) Transition state. (D) Product geometry.

Our analysis shows that Model A fails to reproduce the experimental values without the inclusion of solvation effects, due to its insufficient description of the halide binding site. The gas-phase barrier is about 8 kcal/mol above the experimental value, while the reaction energy indicates that formation of the epoxide is highly endothermic, in contrast with experimental findings. However, with the inclusion of dielectric effects, especially employing large dielectric constants ($\epsilon > 8$), the reaction was found to proceed with a plausible barrier and reaction energy, in agreement with experimental results. Thus, despite its relative smallness, Model A provides support to the concerted mechanism shown in Scheme 2.

The poor description of the halide binding site makes the solvation effects in Model A very large, amounting to more than 14 kcal/mol for the reaction energy using $\epsilon = 4$. To test the validity and reliability of the above results, we therefore devised two larger models (referred to as Model B and Model C, respectively), in which the halide binding site was successively increased.

III.b. Model B. Model B consists of 112 atoms and contains, in addition to Model A, parts of Pro175, Asn176, Tyr177, Leu178, and Phe12, which gives a better description of the halide binding site (see Figure 3).

In the reactant structure, the chloride of RCPE forms hydrogen bonds as before to the water molecule and the backbone amide of Leu178. In addition, a hydrogen bond between Cl and the backbone of Tyr177 is observed (Figure 3B). The alcohol oxygen forms hydrogen bonds to Ser132 and Tyr145, as in Model A. At the transition state for epoxide formation (Figure 3C), the critical O−C and C−Cl distances are 1.88 and 2.40 Å, respectively. The alcohol proton is 1.07 Å from Tyr145 and 1.42 Å from the substrate oxygen. The three hydrogen bonds to the chloride have decreased significantly in length compared to the reactant, since the interactions with the partially displaced chloride ion are

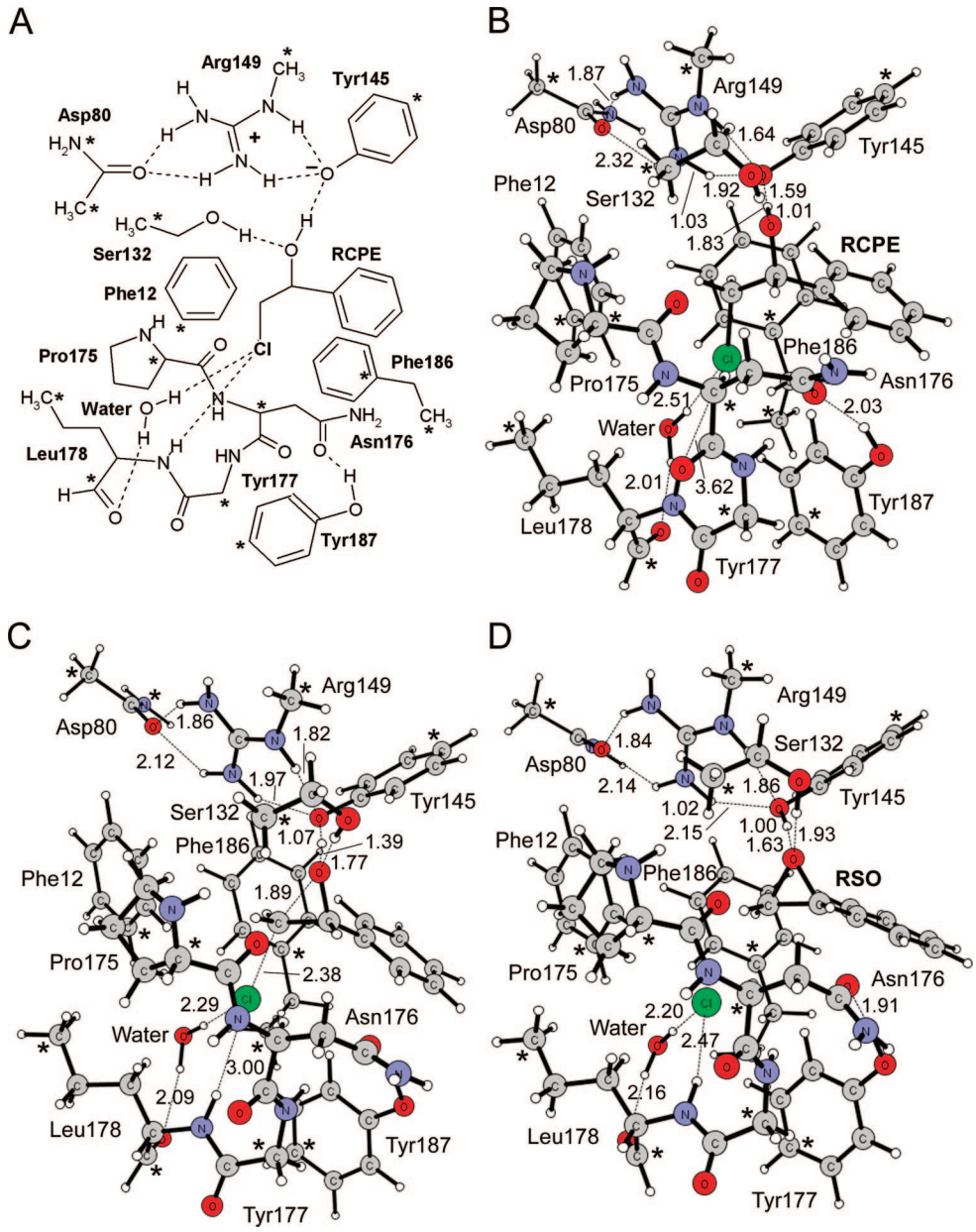

Figure 4. Optimized geometries for the largest model, Model C. (A) Schematic representation of the model. (B) Reactant geometry. (C) Transition state. (D) Product geometry.

stronger than with the neutral side chain. These interactions are further enhanced in the product state (Figure 3D), where the chloride ion has been fully liberated.

The calculated barrier for Model B is 17.9 kcal/mol, and the reaction energy is +14.1 kcal/mol (see Table 1). Both of these values are lower than the ones calculated for Model A (23.0 and 17.5 kcal/mol, respectively). Upon inclusion of solvation effects, both the barrier and the reaction energy decrease further. For example, the barrier decreases to 14.6 and 13.5 kcal/mol using $\epsilon = 4$ and $\epsilon = 80$, respectively, and the reaction energy decreases to +5.2 and +2.2 kcal/mol using $\epsilon = 4$ and $\epsilon = 80$, respectively. Although still very significant, the effects are smaller than for Model A due to the increased size of the halide binding site.

Overall, after consideration of the solvation effects, Model B conveys a very similar picture of the reaction mechanism of HheC to that of Model A.

III.c. Model C. The solvation effect on the reaction energy in Model B is still rather large (8.9 kcal/mol using $\epsilon = 4$, see Table 1), indicating that also this model lacks important parts of the halide binding site. Therefore, we devised an even larger model (referred to as Model C) which consists of 161 atoms and contains in principle the full side chains of the main residues forming the halide binding site, i.e. Pro175, Asn176, Tyr187, Phe12, and Phe186. Also, most of the Leu178 side chain is included (see Figure 4).

In the reactant geometry, the chloride forms hydrogen bonds with the water molecule and with the backbone amide of Leu178 (Figure 4B), but no interaction with the backbone amide of Tyr177 is observed, in contrast to Model B. The optimized transition state for chloride displacement exhibits very similar distances to those of Model B (Figure 4C). The carbon−chloride bond length is 2.38 Å, and the forming carbon−oxygen bond length is 1.89 Å. In the product state,

the liberated chloride ion forms hydrogen bonds to the water molecule and to the backbone of Leu178, but not to the Tyr177 amide (Figure 4D). A possible reason is that the Tyr187 side chain introduced in Model C sterically hinders the chloride from approaching the Tyr177 backbone amide.

The barrier computed for Model C is 18.2 kcal/mol and the reaction energy is +5.5 (Table 1). Since the halide binding site is essentially saturated, the computed solvation effects are very small. For example, in going from no solvation to solvation with $\epsilon = 80$, the barrier drops only by 1.2 kcal/mol and the reaction energy by 1.3 kcal/mol.

Similar to the previous models, the results of Model C demonstrate the energetic feasibility of the proposed reaction mechanism. However, the barrier is slightly overestimated and the reaction energy is positive, in disagreement with experimental results. Several sources for this disagreement can be envisaged. One reason could be that the subsequent regeneration of the anion at the Tyr145 residue through the release of a proton to the bulk is an exothermic process that thus reduces the overall reaction energy. Also, release of the chloride ion could be energetically favorable, which would lower the reaction energy. Moreover, the calculated energies correspond to enthalpies. It is possible that the addition of entropic effects would lower the product state somewhat compared to the reactant state. However, another reason could be due to the chosen model. In Model C, the halide binding site is quite large, and in order to keep it intact in the model, it is necessary to lock a number of centers (indicated by asterisks in Figure 4) such that no artificial hydrogen-bond interactions or large movements take place. This procedure is, many times, very successful, but in the case of Model C, it might have introduced too much strain in the system and, therefore, resulted in a slightly endothermic reaction instead of a slightly exothermic one. Releasing constraints completely, however, is not an option in this model, because it will cause a major disruption to the halide binding site. The various groups will move freely and form artificial hydrogen bonds that are not present in the enzyme. To release the constraints will thus add more uncertainty to the results rather than make them more accurate.

IV. Conclusions

In the present paper, three quantum chemical active site models of different sizes have been employed to investigate the dehalogenation reaction of the haloalcohol dehalogenase HheC enzyme. The computed energies for the three models are summarized in Table 1. The conclusions can be divided into two parts, one related to the specific reaction under study, that is, the HheC reaction mechanism, and one related to the methodology used.

The three models give a consistent picture of the reaction mechanism taking place. The dehalogenation is shown to occur in a single concerted step in which Tyr145 abstracts a proton from the halohydrin substrate and the substrate oxyanion displaces the chloride ion through an intramolecular S_N2 reaction. Arg149 is suggested to activate Tyr145 by abstracting a proton, and Ser132 seems to be of importance for both binding of the substrate and stabilization of the oxyanion at the transition state. The activation barriers and reaction energies calculated for all three models (especially when solvation is considered) show that this reaction mechanism is energetically plausible.

Due to the large solvation energy of free halide ions, dehalogenation reactions are particularly challenging to treat using quantum chemical models in conjunction with implicit solvent. Unless the model is carefully chosen and the surrounding is properly accounted for, small models could yield unrealistic energies. It is here constructive to compare the energies obtained using the three models in order to gain deeper insight into the strengths and shortcomings of this approach.

Model A has a very small halide binding site, consisting of essentially two hydrogen bonds. As expected, the energies obtained with this small model are highly sensitive to the added solvation (see Table 1). Without solvation, this model yields a reaction barrier and energy that are highly overestimated compared to experiments. However, when the implicit solvation is added, this model reproduces the experiments quite nicely. This demonstrates that the implicit solvation model indeed is able to provide a rather good estimation of the solvation effect that the lacking protein surroundings would provide.

Model B provides an improved description of the halide binding site, which is immediately evident from the obtained energies without the solvation added. Both the barrier and the reaction energy are lower than for Model A (without solvation). Also, the solvation effects are smaller than for Model A, but they are still quite large.

For both Model A and Model B, we notice that the solvation effects on the energies saturate very quickly as a function of the dielectric constant (compare, e.g., the values for $\epsilon = 4$ and $\epsilon = 80$ in Table 1). This result can easily be rationalized by considering the simple Onsager model of a dipole in a spherical cavity, for which the solvation energy is proportional to $(\epsilon - 1)/(2\epsilon + 1)$. This simple fact is important to realize when choosing which dielectric constant to use in the modeling of enzymatic reactions (see below).

In Model C, the halide binding site is essentially saturated. This results in energies that are practically the same with and without solvation correction. Hence, the inaccuracy of the approximation of using a homogeneous polarizable continuum model decreases as the model size increases. The further away from the active site the truncation is made, the better this approximation performs, because most of the polarization effects on the reactive parts are already explicitly included in the quantum calculations. However, Model C fails to reproduce the fact that the enzyme−product complex (epoxide + chloride ion) should be more stable than the enzyme−substrate complex (chloroalcohol). As discussed above, this could be due to the proton release step, but most likely it is a result of the locking scheme used.

By comparing the results of Models A and B to those of Model C, one can conclude that a relatively small model of the enzyme active site, in combination with implicit solvent models, can be very useful in studying the enzyme reaction mechanism also for dehalogenation reactions. In fact, larger models could suffer from limitations that smaller models do not have. For example, it is difficult to ensure that different

stationary points are in the same local minima with respect to the parts that are not directly involved in the reaction. In the case of Model C, it was essential to keep a number of atoms fixed to their crystallographic positions in order to avoid that artificial movements of the various groups at the active site take place. This procedure led to a somewhat rigid halide binding site, which resulted in a raised reaction barrier compared to the smaller models. The alternative approach is of course to use QM/MM methods where fixing truncation atoms is not necessary and the flexibility of the surroundings is properly accounted for.[22] However, in QM/MM, it becomes even more difficult to deal with the multiple minima problem.

A final remark concerns the choice of dielectric constant when computing solvent corrections to quantum chemical active site models. Typically, an $\epsilon = 4$ value is used.[13,15] This value is considered to correspond to a mixture of the protein itself (ϵ of 2−3) and water ($\epsilon = 80$).[23] The exact choice is thus somewhat arbitrary.

By comparing the results of Models A and B to those of Model C (Table 1), it can be seen that with $\epsilon = 4$ the various models give results that do not differ much. This shows that the choice of $\epsilon = 4$ works reasonably well. Also, as pointed out above, the solvation energy saturates quickly as a function of ϵ. In going from the cluster model (no solvation) to $\epsilon = 4$, most of the solvation is accounted for. The difference between $\epsilon = 4$ and $\epsilon = 80$ is not very large. For Model A, for example, the energy difference between no solvation and solvation with $\epsilon = 4$ is 14.1 kcal/mol for the reaction energy, while it is only 4.6 kcal/mol between $\epsilon = 4$ and $\epsilon = 80$. For Model B, the corresponding values are 8.9 and 3.0 kcal/mol, respectively. It is very important to point out here that the continuum solvation is an approximation, and the conclusion drawn about reaction mechanisms should not be very sensitive to the exact choice of the dielectric constant or else the approximation cannot be trusted.

Acknowledgment. We gratefully acknowledge financial help from The Swedish Research Council, The Wenner-Gren Foundations, The Carl Trygger Foundation, and The Magn Bergvall Foundation.

References

(1) Nakamura, T.; Nagasawa, T.; Yu, F.; Watanabe, I.; Yamada, H. *Appl. Environ. Microbiol.* **1994**, *60*, 1297–1301.

(2) van den Wijngaard, A. J.; Reuvekamp, P. T. W.; Janssen, D. B. *J. Bacteriol.* **1991**, *173*, 124–129.

(3) van Hylckama Vlieg, J. E. T.; Tang, L.; Lutje Spelberg, J. H.; Smilda, T.; Poelarends, G. J.; Bosma, T.; van Merode, A. E.; Fraaije, M. W.; Janssen, D. B. *J. Bacteriol.* **2001**, *183*, 5058–66.

(4) Fetzner, S.; Lingens, F. *Microbiol. Rev.* **1994**, *58*, 641–685.

(5) Janssen, D. B.; Majerić-Elenkov, M.; Hasnoui, G.; Hauer, B.; Lutje Spelberg, J. H. *Biochem. Soc. Trans.* **2006**, *34*, 291–295.

(6) Majerić-Elenkov, M.; Hauer, B.; Janssen, D. B. *Adv. Synth. Catal.* **2006**, *348*, 579–585.

(7) Lutje Spelberg, J. H.; van Hylckama Vlieg, J. E. T.; Tang, L.; Janssen, D. B.; Kellogg, R. M. *Org. Lett.* **2001**, *3*, 41–43.

(8) Lutje Spelberg, J. H.; Tang, L.; van Gelder, M.; Kellogg, R. M.; Janssen, D. B. *Tetrahedron Asym.* **2002**, *13*, 1083–1089.

(9) Majerić-Elenkov, M.; Tang, L.; Hauer, B.; Janssen, D. B. *Org. Lett.* **2006**, *8*, 4227–29.

(10) Hasnaoui, G.; Lutje Spelberg, J. H.; de Vries, E.; Tang, L.; Hauer, B.; Janssen, D. B. *Tetrahedron Asym.* **2005**, *16*, 1685–1692.

(11) Nakamura, T.; Nagasawa, T.; Yu, F.; Watanabe, I.; Yamada, H. *Biochem. Biophys. Res. Commun.* **1991**, *180*, 124–130.

(12) de Jong, R. M.; Tiesinga, J. J.; Rozeboom, H. J.; Kalk, K. H.; Tang, L.; Janssen, D. B.; Dijkstra, B. W. *EMBO J.* **2003**, *22*, 4933–44.

(13) See for example the following reviews: (a) Blomberg, M. R. A.; Siegbahn, P. E. M. *J. Phys. Chem. B* **2001**, *105*, 9375. (b) Himo, F.; Siegbahn, P E. M. *Chem. Rev.* **2003**, *103*, 2421. (c) Siegbahn, P. E. M. *Q. Rev. Biophys.* **2003**, *36*, 91. (d) Noodleman, L.; Lovell, T.; Han, W.-G.; Li, J.; Himo, F. *Chem. Rev.* **2004**, *104*, 459. (e) Himo, F. *Biophys. Biochim. Acta* **2005**, *1707*, 24. (f) Himo, F. *Theor. Chem. Acc.* **2006**, *116*, 232.

(14) (a) Lee, C.; Yang, W.; Parr, R. G. *Phys. Rev. B: Condens. Matter Mater. Phys.* **1988**, *37*, 785–89. (b) Becke, A. D. *Phys. Rev. A: At., Mol., Opt. Phys.* **1988**, *38*, 3098–3100. (c) Becke, A. D. *J. Chem. Phys.* **1992**, *96*, 2155–2160. (d) Becke, A. D. *J. Chem. Phys.* **1992**, *97*, 9173–77. (e) Becke, A. D. *J. Chem. Phys.* **1993**, *98*, 5648–52.

(15) (a) Velichkova, P.; Himo, F. *J. Phys. Chem. B* **2005**, *109*, 8216. (b) Himo, F.; Guo, J.-D.; Rinaldo-Matthis, A.; Nordlund, P. *J. Phys. Chem. B* **2005**, *109*, 20004. (c) Velichkova, P.; Himo, F. *J. Phys. Chem. B* **2006**, *110*, 16. (d) Chen, S.-L.; Fang, W.-H.; Himo, F. *J. Phys. Chem. B* **2007**, *111*, 1253. (e) Sevastik, R.; Himo, F. *Bioorg. Chem.* **2007**, *35*, 444. (f) Hopmann, K. H.; Guo, J.-D.; Himo, F. *Inorg. Chem.* **2007**, *46*, 4850.

(16) Hopmann, K. H.; Hallberg, B. M.; Himo, F. *J. Am. Chem. Soc.* **2005**, *127*, 14339.

(17) (a) Hopmann, K. H.; Himo, F. *Chem.—Eur. J.* **2006**, *12*, 6898. (b) Hopmann, K. H.; Himo, F. *J. Phys. Chem. B.* **2006**, *110*, 21299.

(18) (a) Hur, S.; Kahn, K.; Bruice, T. C. *Proc. Natl. Acad. Sci. U. S. A.* **2003**, *100*, 2215–9. (b) Lau, E. Y.; Kahn, K.; Bash, P. A.; Bruice, T. C. *Proc. Natl. Acad. Sci. U. S. A.* **2000**, *97*, 9937–42. (c) Lightstone, F. C.; Zheng, Y. J.; Maulitz, A. H.; Bruice, T. C. *Proc. Natl. Acad. Sci. U. S. A.* **1997**, *94*, 8417–20. (d) Lightstone, F. C.; Zheng, Y.-J.; Bruice, T. C. *J. Am. Chem. Soc.* **1998**, *120*, 5611–5621.

(19) Frisch, M. J.; Trucks, G. W.; Schlegel, H. B.; Scuseria, G. E.; Robb, M. A.; Cheeseman, J. R.; Montgomery, J. A., Jr.; Vreven, T.; Kudin, K. N.; Burant, J. C.; Millam, J. M.; Iyengar, S. S.; Tomasi, J.; Barone, V.; Mennucci, B.; Cossi, M.; Scalmani, G.; Rega, N.; Petersson, G. A.; Nakatsuji, H.; Hada, M.; Ehara, M.; Toyota, K.; Fukuda, R.; Hasegawa, J.; Ishida, M.; Nakajima, T.; Honda, Y.; Kitao, O.; Nakai, H.; Klene, M.; Li, X.; Knox, J. E.; Hratchian, H. P.; Cross, J. B.; Adamo, C.; Jaramillo, J.; Gomperts, R.; Stratmann, R. E.; Yazyev, O.; Austin, A. J.; Cammi, R.; Pomelli, C.; Ochterski, J. W.; Ayala, P. Y.; Morokuma, K.; Voth, G. A.; Salvador, P.; Dannenberg, J. J.; Zakrzewski, V. G.; Dapprich, S.; Daniels, A. D.; Strain, M. C.; Farkas, O.; Malick, D. K.; Rabuck, A. D.; Raghavachari, K.; Foresman, J. B.; Ortiz, J. V.; Cui, Q.; Baboul, A. G.; Clifford, S.; Cioslowski, J.; Stefanov, B. B.; Liu, G.; Liashenko, A.; Piskorz, P.; Komaromi, I. ;

Martin, R. L.; Fox, D. J.; Keith, T.; Al-Laham, M. A.; Peng, C. Y.; Nanayakkara, A.; Challacombe, M.; Gill, P. M. W.; Johnson, B.; Chen, W.; Wong, M. W.; Gonzalez, C.; Pople, J. A. *Gaussian 03*, revision B.03; Gaussian, Inc.: Pittsburgh, PA, 2003.

(20) (a) Klamt, A.; Schüürmann, G. *J. Chem. Soc., Perkin Trans.* **1993**, *2*, 799–805. (b) Andzelm, J.; Kölmel, C.; Klamt, A. *J. Chem. Phys.* **1995**, *103*, 9312–9320. (c) Barone, V.; Cossi, M. *J. Phys. Chem. A* **1998**, *102*, 1995–2001. (d) Cossi, M.; Rega, N.; Scalmani, G.; Barone, V. *J. Comput. Chem.* **2003**, *24*, 669–681.

(21) Tang, L.; Lutje Spelberg, J. H.; Fraaije, M. W.; Janssen, D. B. *Biochemistry* **2003**, *42*, 5378–5386.

(22) For a recent comprehensive review on QM/MM methods for biological systems, see:(a) Senn, H. M.; Thiel, W. *Top. Curr. Chem.* **2007**, *268*, 173.

(23) Siegbahn, P. E. M.; Blomberg, M. R. A. *Chem. Rev.* **2000**, *100*, 421–437.

CT8000443